Growth of funnel-shaped GaN nanowire by switching the growth mode between VLS/VS

Y. ZHANG[1,*], Y. ZONG[2,*], J. HUANG[1], W. L. LIU[3]
[1]*School of Intelligent and Electronic Engineering, Dalian Neusoft University of Information, Dalian 116000, China*
[2]*School of Information Science and Engineering, Shenyang University of Technology, Shenyang 110000, China*
[3]*School of College of Health and Medical Technology, Dalian Neusoft University of Information, Dalian 116000, China*

Funnel-shaped GaN nanowire(NW) was grown on GaN(0001) coated sapphire substrate with Ni/Au catalyst by using MOCVD. The catalyst thickness and III-V ratio were investigated to control the NW growth mode. By changing the catalyst thickness to tuning the catalyst droplet surface energy, and the III-V ratio to form different chemical potential of the gaseous reactants, the NW growth mode can vary between VLS and VS. Funnel-shaped GaN NW was obtained through VLS/VS mixed growth mode by using a two-step growth method.

(Received May 29, 2024; accepted December 2, 2024)

Keywords: GaN nanowire, Funnel-shaped, VL/VLS mix mode, Catalyst, III-V ratio

1. Introduction

Due to excellent electrical properties and thermal/chemical stabilities, GaN NW has always been a promising material for semiconductor devices [1-4]. Especially in light emitting [5-7] and light trapping [8-11] area. The morphology of NW has an important impact on its properties. For example, engineering of the NW shapes has been used to increase the light trapping ability [12]. Some report [12-15] that a funnel-shaped Si NW shows strong broadband absorption of the solar spectrum due to different radius in the axial direction, which increases the number of resonance wavelengths. So, understanding the NW shape modulate mechanism may enhance its performance in device [16-17].

There are many reports on the growth of GaN NW. The common method including CVD [18-19] and MOCVD techniques. Some special method such as nitriding the Ga_2O_3 nanobelts into GaN NWs can also be used [20]. There are many factors can affect the nanowires morphology. The type of substrate was found to be a crucial factor in the synthesis of GaN NW [21]. it affects the shape as well as the diameter of the formed nanowires. The NH_3 gas flow rate during the growth can change the morphology of GaN from thin film to different morphologies of nanostructures [22]. The ammoniating can help to obtain good quality and high density of NWs with diameters around 50 nm and lengths up to tens of microns [23]. However, there is no previous report on the growth of funnel-shaped GaN NW.

In this paper, the growth conditions including the catalyst thickness and III-V ratio which are factors influencing the NW growth mode were discussed. And a two-step growth method was proposed to obtain funnel-shaped GaN NW by switching the growth mode between VS and VLS.

2. Experiment

Sapphire substrate with 3μm thick (0001) gallium nitride film was used to grow GaN NW. The gallium nitride thin films can reduce lattice mismatch and defects, resulting in excellent crystal quality NW due to the same lattice constant and thermal expansion coefficient. Meanwhile, with the electric conductivity, this thin film can be used as bottom electrodes in future device fabrication [24]. Thin films of nickel and gold materials were prepared on the substrate surface using magnetron sputtering method [25], and used as catalysts to grow NW following the VLS mechanism. A cold-walled horizontal-flow MOCVD system was employed. Trimethylgallium (TMGa) and NH3 were used as sources, and N2/H2 (with 5% H2) was employed as carrier gas. The pressure stabilized at 300Torr during growth.

As listed in Table 1, 4 kinds of NW samples M1-M4 were prepared under different conditions. Sample M5 was grown using a two-step method to obtain funnel-shaped NW, its growth parameters are listed in Table 2.

Table 1. Growth parameters of GaN nanowire samples M1-M4

Sample	Ni/Au thickness (nm)	Growth parameters			
		Tn(℃)	TMGa(sccm)	NH_3(sccm)	Time(s)
M1	5/5	750	2	20	800
M2	2/2	750	2	20	800
M3	5/5	750	3	20	800
M4	5/5	750	4	20	800

Table 2. Growth parameters of GaN nanowire sample M5

Sample	Ni/Au thickness (nm)	1st-step				2nd-step			
		Tn (℃)	TMGa (sccm)	NH_3 (sccm)	Time (s)	Tg (℃)	TMGa (sccm)	NH_3 (sccm)	Time (s)
M5	5/5	750	4	20	800	750	2	20	200

3. Result and discussion

3.1. Characterization

Catalyst plays a crucial role in the preparation of GaN NW following the VLS mechanism [26-29]. The distribution of droplets formed by the catalyst under high temperature determines the positions of saturated precipitated GaN crystals. The size of the catalyst droplets determines the geometric size of NW growth. In this paper, two different thickness Ni/Au catalysts were used to prepare two sets of GaN NW samples at the same temperature and III-V ratio. The specific growth parameter settings are shown in Table 1. The SEM images of the NW grown in samples M1 and M2 are shown in Fig. 1.

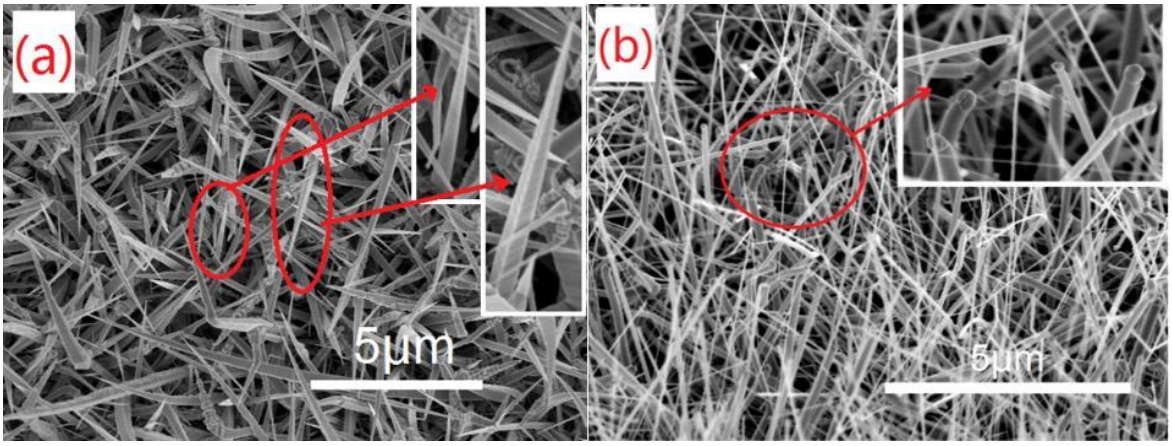

Fig. 1. SEM images of samples M1-M2 (color online)

As shown in Fig. 1, there are differences in the morphology of the two groups of NW. The NW in sample M1 exhibits a prism shaped morphology, as shown in Fig. 1 (a), with a thicker bottom diameter that can reach 800nm. And the top gradually becomes thinner, with a tip diameter less than 50nm and an average length of 5 μm. The morphology in sample M2 is shown in Fig. 1 (b), all of which are smooth cylindrical structures. The diameter distribution is relatively uniform, with an average diameter of about 150nm. The NW is slender and straight, with a length of up to 10 μm above.

The growth conditions of samples M1 and M2 were the same, except for the difference in catalyst thickness. Therefore, it can be inferred that the differences in the morphology is caused by the different catalyst thickness. By carefully observing the morphology of the NW in sample M1, the tip of the prism NW in M1 is very sharp, and no trace of catalyst particles can be found at the tip. Therefore, it is speculated that due to the large thickness of the catalyst in sample M1, it is not possible to form small enough catalyst droplets at high temperature. Therefore, the Ni/Au film did not truly act as a catalyst during the growth process. The NW might not nucleate and precipitate from the catalyst droplets, or the catalyst droplets might slip off the top of the NW during the growth process. The growth mode of NW in sample M1 is not VLS mechanism, but follows VS growth mechanism.

The morphology of prism NW in sample M1 can also reveal traces of VS growth. Two NWs with different lengths are selected in the illustration of Fig. 1 (a). The diameter and length of both are not the same, but the angle of the top sharp corner is basically the same, both around 9 °. This

indicates that the NW not only undergo axial growth during the growth process, resulting in a longer length; At the same time, it also undergoes radial growth, causing them to continuously thicken, thus ensuring that the angle of the top sharp corner remains unchanged. And the radial growth is the main characteristic of VS growth mechanism.

For the NW in sample M2, the catalyst particles at the top of the NW can be clearly seen from the illustration in Fig. 1 (b), indicating that the growth of the NW in sample M2 followed the VLS growth mechanism. GaN crystals precipitate below the catalyst droplets, increasing the length of the NW without radial growth. The diameter of the NW remains unchanged, presenting a slender cylindrical shape.

Therefore, the thickness of the catalyst film can alter the growth mechanism. Thick catalysts (such as 10nm) cannot form sufficient small catalyst droplets after annealing, and NW will follow the VS mechanism in growth. NW grows simultaneously in both axial and radial directions, which can be used to prepare radial heterojunction NW structures. Thin catalysts (such as 4nm) can form smaller enough catalyst droplets, and NW will grow according to the VLS mechanism. During the growth process, the NW only undergo axial growth, resulting in cylinder NW with uniform diameter, which can be used to prepare axial heterojunction NW structures.

3.2. The effect of catalyst thickness on growth mode

When preparing GaN NW using the MOCVD method, the growth process of the NW is result of competition between the VS and VLS mechanism [30-32]. During this process, the thickness of the catalyst plays a crucial role [33], resulting in completely different morphology of the NWs in samples M1 and M2. The mechanism of the catalyst's influence will be discussed below.

Considering the nucleation process of NW in VLS growth mechanism based on thermodynamic and kinetic principles [34], the Gibbs free energy changes of the entire system before and after the nucleation reaction can be obtained in equation1. This includes the reduction of free energy during the transformation of gaseous reactants into liquid phase, the increase in surface free energy caused by the formation of liquid crystal nuclei, and the interface free energy generated by the formation of solid-liquid interfaces with the substrate surface [35]. By analyzing the changes in Gibbs free energy of the system, the direction of the reaction can be determined and whether the nucleation process of NW can proceed.

$$\Delta G = -\frac{4}{3}\pi R^3 \frac{(1-\cos\theta)^2(2+\cos\theta)}{4}\frac{\Delta\mu}{v_l} + 2\pi\sigma R^2(1-\cos\theta) - \pi\sigma R^2(\sin\theta)^2\cos\theta \quad (1)$$

By taking the derivative of equation (1) over R, we can obtain:

$$R_{limit} = \frac{2\sigma v_l}{\Delta\mu} \quad (2)$$

R_{limit} is the critical radius for the nucleation of NW. During the nucleation process, when the nuclei radius is less than the critical radius R_{limit}, the Gibbs free energy of the system will increase with the crystal nuclei radius, causing the system to become unstable, the crystal nuclei will vaporize and disappear. When the nuclei radius is greater than the critical radius R_{limit}, it is necessary to consider the relationship between the chemical potential of gas phase reactants and crystal nuclei. Givargizov et al. [36] explored the growth rate of NW based on experimental data also lead to the same R_{limit}.

When growing the NW follow VLS mechanism, various factors need to be considered such as the chemical potential of gaseous reactants, the free energy of the substrate surface, and the surface energy of catalyst droplets to determine whether NW growth can happen [37]. The surface energy of catalyst droplets is related to the radius of the droplets, larger radius leads to the higher surface energy. When the radius of the catalyst droplet exceeds the critical radius R_{limit}, it is necessary to control the chemical potential of the gaseous reactant to be greater than the surface energy of the catalyst droplet in order to reduce the Gibbs free energy of the system and allow the reaction to proceed. At this point, if the catalyst thickness is not thick enough, the surface energy of the droplets formed is lower than the chemical potential of the gaseous reactants, the NW can grow according to the VLS mechanism, resulting in cylindrical NW like those in sample M2.

When the III-V ratio and pressure remain constant, the chemical potential of the gaseous reactants in the system will remain unchanged [38]. At this point, increasing the radius of the catalyst droplet will result in an increase in its surface energy. When the radius of the catalyst droplet increases to a certain extent, its surface energy will be greater than the chemical potential of the gaseous reactant, which will prevent the nucleation reaction from proceeding. Therefore, when the thickness of the catalyst film is too large, the NW will not be able to grow according to the VLS mechanism. When other conditions in the system are suitable, the NW will grow in VS mode, and sample M1 fits this situation, resulting in a prism shaped NW.

Therefore, when the radius of the catalyst droplet is too large, it is necessary to increase the chemical potential of the gaseous reactants in order for the NW to grow in VLS mode. To verify this conclusion, other two samples M3 and M4 were prepared. These two samples were using the same thickness catalyst film as sample M1, maintained the flow rate of ammonia unchanged and increased the flow rate of gallium source, thereby the chemical potential of gaseous reactants was enhanced. The growth parameters are shown in Table 1.

The SEM images of NW obtained in samples M3 and M4 are shown in Fig. 2. When the III-V ratio increased to 3:20, most of the NWs in sample M3 still grown in VS mode, but few NWs have already grown in VLS mode. As shown in the enlarged image in Fig. 2 (a), catalyst particles with a diameter of approximately 500nm can be seen at the

top of the NW. The NW exhibits a prism shaped morphology, and a large number of radial growth traces can be seen on the sidewalls. Therefore, this type of NW is a product of the combination of VLS and VS modes, which nucleated in the catalyst and followed the VLS mechanism for axial growth; At the same time, radial growth was carried out on the bottom and side walls in VS mode, resulting in a prism shaped NW with a thick bottom, and a small top with the catalyst particles on it. When the III-V ratio continued to increase to 4:20, it can be seen from Fig. 2 (b) that the quantity of NWs grown in this mode increased. At the same time, due to the non-uniformity of the droplet diameter formed by the catalyst at high temperature, the size of the catalyst particles at the top of the NW also varied, with a maximum diameter of 500nm and a minimum diameter of only about 50nm.

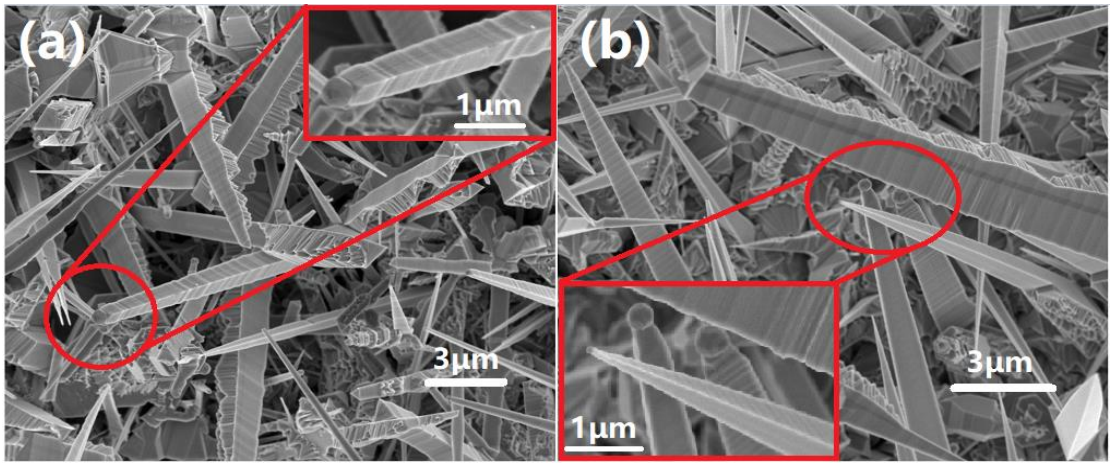

Fig. 2. SEM images of samples M3-M4 (color online)

The growth results indicate that when the gas reaction flow rate is increased, the chemical potential of the gas reactants will be greater than the surface energy of the catalyst droplets. At this time, 10nm Ni/Au catalyst can also nucleate and grow NW in VLS mode. Therefore, as shown in Fig. 3, during the growth process, the thickness of the catalyst and the III-V ratio of the reaction gas will both affect the growth mode of the NW. When the catalyst is thin (4nm), a lower III-V ratio (2:20) can be used for VLS growth. When the III-V ratio reaches 2:40, the NW shifts towards VS growth; When the catalyst is thicker (10nm), a higher III-V ratio (4:20) is required for VLS growth. When the III-V ratio decreases to 2:20, the NW shifts towards VS growth.

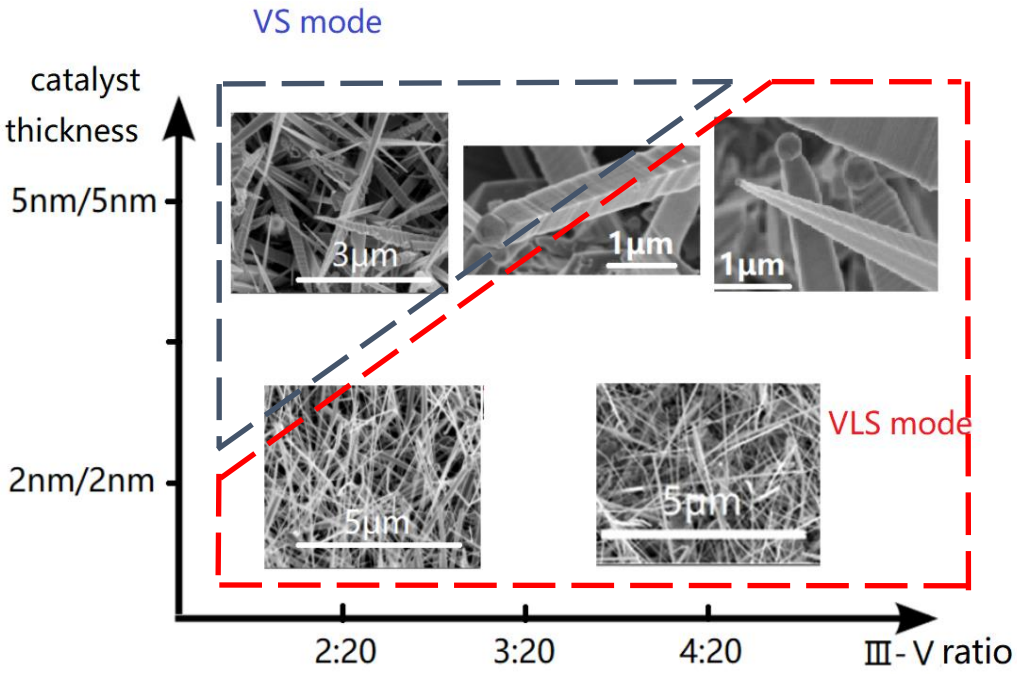

Fig. 3. Influence of catalyst thickness and III-V ratio on growth mode (color online)

3.3. Synthesis of funnel-shaped NW

Based on the above experimental results, this paper further proposes a "funnel-shaped" GaN NW and its preparation method. On the basis of the prism shaped NWs with catalyst particles on the top in samples M3 and M4, a two-step growth process was adopted. By changing the growth conditions and utilizing the catalyst particle at the top of the NW, cylindrical NW can be further grown on the substrate of prism NW, which resulting in a "funnel-shaped" NW structure.

The growth parameters of sample M5 are shown in Table 2. Firstly, a thicker diameter prism shaped NW "base" was prepared using the same growth conditions of sample M4, with a bottom diameter of up to 1 μm. Then, lower the III-V ratio and use the growth conditions of sample M2 to continue the growth on the prism NW following the VLS mechanism, resulting in slender cylindrical NW with a diameter of approximately 50nm on the prism shaped NW "base". A GaN NW structure resembling an inverted "funnel" was obtained, as shown in Fig. 4. The XRD result is shown in Fig. 5.

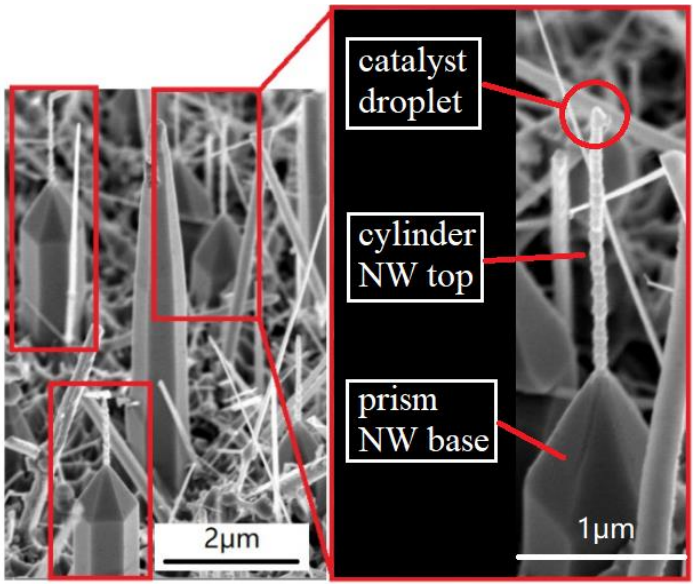

Fig. 4. SEM images of sample M5 (color online)

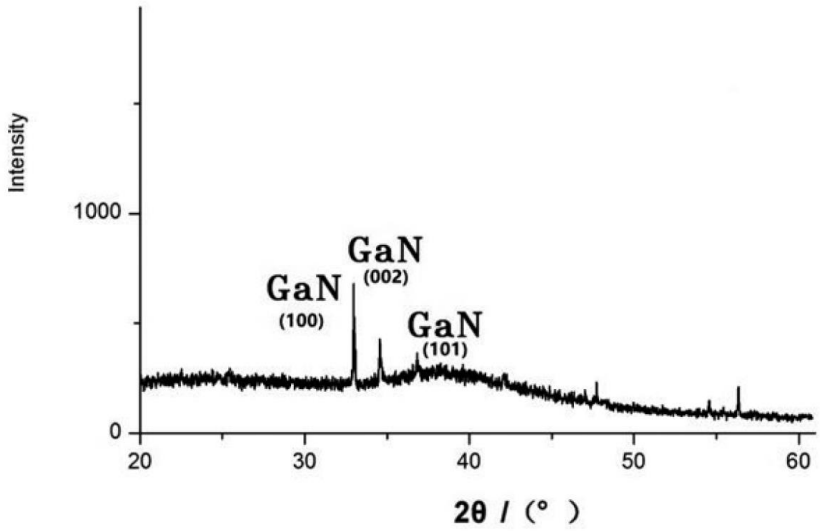

Fig. 5. XRD result of sample M5

The "funnel-shaped" NW has a large bottom radius and can form good electrical contact with the substrate. At the same time, the upper radius is small, and the ratio to the bottom can reach 1:20. Due to the limitation effect of quantum size, the bandgap width of NW increases with the decrease of radius. Therefore, there is a difference in the bandgap width between the upper and lower parts of this "funnel-shaped" NW, which has certain advantages in

forming NW junction devices. moreover, its unique geometric morphology can enhance the electron emission and light trapping characteristics, providing new possibilities for its application in various fields.

4. Conclusions

In summary, funnel-shaped GaN NW was grown by a MOCVD method using Ni/Au as catalyst. The growth mode of NW can be varied by control the catalyst thickness and III-V ratio. When the catalyst is thicker (10nm), a higher III-V ratio (4:20) is required for VLS growth, otherwise the NWs shift towards VS growth. A two-step method is applied to manipulate the growth mode in different stage to obtain the funnel-shaped NW, and the radius ratio of the upper and lower parts can reach 1:20.

References

[1] R. R. Thakur, N. Chaturvedi, Materials Today: Proceedings **80**, 2232 (2023).
[2] R. R. Thakur, N. Chaturvedi, Semiconductor Science and Technology **6**(7), 075013 (2021).
[3] X. Tang, Y. Zheng, B. Cao, Q. Wu, J. H. Liang, W. L. Wang, G. Q. Li, ACS Applied Nano Materials **5**(3), 4515 (2022).
[4] M. A. A. Z. M. Sahar, Z. Hassan, S. S. Ng, N. A. Hamzah, Materials Science in Semiconductor Processing **156**(15), 107298 (2023).
[5] M. Takiguchi, S. Sergent, B. Damilano, S. Vézian, S. Chenot, N. Yazigi, P. Heidt, T. Tsuchizawa, T. Yoda, H. Sumikura, A. Shinya, M. Notomi, ACS Photonics **11**(2), 789 (2024).
[6] J. T. Qu, R. J. Wang, P. Pan, L. H. Du, Y. Sun, X. Y. Liu, Nanoscale **15**(12), 5671 (2023).
[7] F. Lu, L. Liu, J. Tian, X. Zhangyang, H. Cheng, X. Guo, Materials Science and Engineering B **282**, 115795 (2022).
[8] A. V. J. P. Aissa, Optik **207**, 163844 (2020).
[9] P. Ji-Hyeon, R. Nandi, S. Jae-Kwan, U. Dae-Young, K. San. K. Jin-Soo, L. Cheul-Ro, RSC Advances **8**(37), 20585 (2018).
[10] K. M. A. Saron, M. Ibrahim, T. A. Taha, A. I. Aljameel, A. G. Alharbi, A. M. Alenad, B. A. Alshammari, G. Almutairi, N. K. Alam, Solar Energy **227**, 525 (2021).
[11] M. B. E. Robin, E. Robin, ACS Applied Nano Materials **6**(14), 12792 (2023).
[12] M. Hussein, M. F. O. Hameed, N. F. F. Areed, A. Yahia, S. S. A. Obayya, Optics Letters **41**(5), 1010 (2016).
[13] Ghada Yassin Abdel-Latif, Mohamed Farhat O. Hameed, Mohamed Hussein, Maher Abdel Razzak, Salah S. A. Obayya, Journal of Photonics for Energy **7**(4), 047501 (2017).
[14] Zoheir Kordrostami, Ali Yadollahi, Optics Communications **459**, 125059 (2020).
[15] D. P. Wilson, A. S. Sokolovskii, N. I. Goktas, V. G. Dubrovskii, R. R. LaPierre, IEEE Journal of Photovoltaics **9**(5), 1225 (2019).
[16] S. Wang, P. Shao, T. Zhi, Z. Gao, W. Chen, L. Hao, Q. Cai, J. Wang, J. Xue, B. Liu, Advanced Photonics Nexus **2**(3), 036003 (2023).
[17] F. Lu, L. Liu, J. Tian, Y. X. Zhang, H. Cheng, X. Guo, Physica Status Solidi: Rapid Research Letters **16**(12), 2200305 (2022).
[18] Q. N. Abdullah, F. K. Yam, J. J. Hassan, C. W. Chin, Z. Hassan, M. Bououdina, International Journal of Hydrogen Energy **38**(32), 14085 (2013).
[19] Q. N. Abdullah, F. K. Yam, Z. Hassan, M. Bououdina, Journal of Colloid and Interface Science **460**, 135 (2015).
[20] F. K. Yam, Z. Hassan, M. Bououdina, Superlattices and Microstructures **54**, 215 (2013).
[21] Q. N. Abdullah, F. K. Yam, N. K. Hassan, M. A. Qeed, K. Al-Heuseen, M. Bououdina, Z. Hassan, Ceramics International **40**(7 PART A), 9563 (2014).
[22] Q. N. Abdullah, F. K. Yam, Z. Hassan, M. Bououdina, Sensors and Actuators B: Chemical **204**, 497 (2014).
[23] Q. N. Abdullah, A. R. Ahmed, A. M. Ali, F. K. Yam, Z. Hassan, M. Bououdina, M. A. Almessiere, Superlattices and Microstructures **117**, 92 (2018).
[24] M. Taisei, T. Tatsuo, U. Masato, Journal of Vacuum Science and Technology A : Vacuum, Surfaces, and Films **40**(5), 053001 (2022).
[25] M. A. Kulkarni, A. Abdullah, H. Thaalbi, F. S.-W. R. Tariq, H. Ryu, S. H. Lee, H. Lim, Optical Materials **145**, 114488 (2023).
[26] V. Purushothaman, K. Jeganathan, Journal of Nanoparticle Research **15**(7), 1789 (2013).
[27] W.-C. Hou, L.-Y. Chen, W.-C. Tang, F. C. N. Hong, Crystal Growth and Design **11**(4), 990 (2011).
[28] U. Saleem, H. Wang, D. Peyrot, A. Olivier, J. Zhang, P. Coquet, S. L. G. Ng, Journal of Crystal Growth **439**, 28 (2016).
[29] D. Zhao, H. Huang, H. Wu, M. Ren, H. Zhu, Y. Liu, B. Sun, Physica Status Solidi A : Applications and Materials Science **210**(12), 2689 (2013).
[30] Y. Liu, X. Meng, Journal of Materials Science: Materials in Electronics **27**(2), 1590 (2016).
[31] V. Purushothaman, V. Ramakrishnan, K. Jeganathan, RSC Advances **2**(11), 4802 (2012).
[32] X. Wan, X.-Q. Meng, Y.-G. Liu, Journal of Functional Materials **45**(2), 2082 (2014).
[33] J. P. Ah, H. Behmenburg, C. Giesen, I. Regolin, W. Prost, F. J. Tegude, G. Z. Radnoczi, B. Pecz, H. Kalisch, R. H. Jasen, M. Heuken, Phys. Status Solidi C **8**, 2315 (2011).
[34] A. Shalabny, F. Buonocore, M. Celino, L. Zhang, K. Sardashti, M. Harth, D. W. Schubert, M. Y. Bashouti, Applied Surface Science **599**, 153957 (2022).
[35] G. T. Wang, A. A. Talin, D. J. Werder, J. Randall,Creighton, E. Lai, R. J. Anderson, I. Arslan, Nanotechnology **17**(23), 5773 (2006).
[36] E. I. Givargizov, Journal of Crystal Growth **52**(part-P1), 194 (1981).

[37] X. T. Hu, Y. M. Song, Z. L. Su, H. Q. Jia, W. X. Wang, Y. Jiang, Y. F. Li, H. Chen, Chinese Physics B **31**(3), 38103 (2022).

[38] M. Taib, S. N. Waheeda, N. Zainal, International Journal of Nanotechnology **19**(2-5), 327 (2022).

*Corresponding author: zhangying@neusoft.edu.cn; zongyang@sut.edu.cn